JOURNAL OF GEOPHYSICAL RESEARCH, VOL. 96, NO. A12, PAGES 21,361–21,369, DECEMBER 1, 1991

# Occurrence Characteristics of VLF Bursts in the Nightside Ionosphere of Venus

C.-M. HO, R. J. STRANGEWAY, AND C. T. RUSSELL

*Institute of Geophysics and Planetary Physics, University of California, Los Angeles*

Many of the impulsive VLF signals observed by the Pioneer Venus orbiter electric field detector (OEFD) in the nightside ionosphere have been interpreted as arising from lightning in the Venus atmosphere. In order to determine the characteristics of the source, and to compare with terrestrial lightning, we determine the normalized occurrence rate for individual bursts at Venus, as opposed to previous studies of activity in 30-s intervals. We establish burst identification criteria which take into account the decay constant of the instrument to calculate the burst rate. Under the assumption that all OEFD observations in the nightside ionosphere are due to impulsive signals, we find that the 100-Hz channel has the highest burst rate, about 0.20/s in the altitude range 150–180 km and in the postmidnight local time sector. The burst occurrence rates for all four frequency channels decrease with increasing altitude. Burst rates at frequencies above 100 Hz are greater in the premidnight hours while 100-Hz signals peak after midnight; however, these burst rates vary from orbit to orbit. The 100-Hz low-frequency burst rate has a stronger dependence on the magnetic field strength than the higher-frequency rates. Most 100-Hz bursts are closely spaced and occur independently of signals at higher frequencies. These dependences suggest that the low- and high-frequency signals have different propagation mechanisms. The properties of the bursts are generally consistent with a lightning source, and the planet-wide burst rate at Venus may be comparable to or larger than the terrestrial lightning rate.

## 1. INTRODUCTION

An important discovery of the Pioneer Venus orbiter electric field detector (OEFD) was the existence of many VLF impulsive signals in the nightside ionosphere. This phenomenon has received much attention and has been extensively studied by many authors [*Taylor et al.*, 1979; *Scarf et al.*, 1980b, 1987; *Scarf and Russell*, 1983; *Singh and Russell*, 1986; *Russell et al.*, 1988a, b, c, 1989a, b, 1990; *Russell*, 1991; *Russell and Scarf*, 1990; *Strangeway*, 1991]. Since the signals are frequently detected at the lowest altitudes around periapsis and have characteristics expected for lightning, that is intense, highly impulsive, and broadband, they have been generally assumed to be generated by lightning or atmospherics. In addition, VLF signals generated by lightning may propagate to a higher altitude in the ionosphere as whistler mode waves. These waves are usually observed only below the gyrofrequency. In the few examples whose polarization was studied the polarization is perpendicular to the ambient magnetic field [*Scarf and Russell*, 1988]. These signals are also often observed in regions of low or variable electron densities [*Scarf et al.*, 1980b].

Pioneer Venus OEFD evidence for lightning was first reported by *Taylor et al.* [1979]. Subsequently, *Scarf et al.* [1980b] discussed in more detail the properties of the impulsive signals and made a strong argument that these signals are generated in the atmosphere and propagate to the spacecraft as whistler mode waves. In their early analyses, Scarf and coworkers used a conservative definition of a possible lightning-generated signal, restricting their analysis to those impulsive signals at 100 Hz below the electron gyrofrequency which were not accompanied by any signals at higher frequencies. To be classed as an event the 100-Hz signals had to have an intensity at least 1 order of magnitude greater than instrument background, and each event could consist of several closely spaced impulsive bursts [*Scarf and Russell*, 1988]. Thus, with this event definition, they excluded broadband events which could be due to Doppler-shifted ion acoustic waves.

Using data from 1185 orbits *Scarf and Russell* [1983] noted that the most active 5° × 5° square area of planetary latitude and longitude had a total of only 24 events. When determining the areal distribution of events, each event was assigned a point on the planetary surface by projection along the magnetic field measured at the spacecraft at the time of the event. The magnetic field at the spacecraft projected into the 5° × 5° area for a total duration of about 1000 s. This yielded a rate of 2.7 bursts/km$^2$/terrestrial year. However, this rate probably underestimates the actual burst rate since many bursts may occur in a single event, and also many bursts were not counted because they failed to meet the conservative criteria. Later, *Scarf et al.* [1987] analyzed a larger sample of data consisting of orbits from the first 9.5 seasons of nightside periapsis and used a more liberal definition of a burst which produced higher burst counts. Even so, they were unable to get an accurate flash rate since the data were not normalized by observing time.

*Singh and Russell* [1986] showed that the signals above the electron gyrofrequency acted very much like those below the electron gyrofrequency. Thus they proposed that these signals had the same source as the 100-Hz signals and could be partially transmitted into the ionosphere in the presence of an ionospheric irregularity, especially when these signals came from a near source and were strong enough. They found that signals were prevalent at all frequencies near periapsis, not just at 100 Hz. However, their results were qualitative and included some telemetry noise [*Taylor and Cloutier*, 1988; *Russell and Singh*, 1989]. Furthermore, they could not be used to determine the signal occurrence rates because their studies did not normalize the events by observing time. Thus none of the early studies provided a correct distribution of occurrence rate in space or time because the length of time spent by the spacecraft in each region was not noted.

*Russell et al.* [1988a] first undertook a normalized occurrence study which measured the activity in every 30-s interval and



Paper number 91JA01980.
0148-0227/91/91JA-01980$05.00

checked whether or not burst activity was present. If the signal reached at least one well-defined maximum within the 30 s, the interval was considered to be active. The percent occurrence rate was calculated by dividing the number of intervals containing bursts by the total number of observing intervals in bins, defined by ranges in local time, longitude, and altitude. They examined the data at all four frequencies sampled by the OEFD at 100 Hz, 730 Hz, 5.4 kHz, and 30 kHz for the first four nightside periapsis seasons of the Pioneer Venus orbiter (PVO) mission. Some important results were obtained on the basis of this and subsequent studies [*Russell et al.*, 1988b, c, 1989a, b, 1990]. The rate of activity decreases rapidly with altitude for those bursts with frequencies above the gyrofrequency, while the rate decreases slowly for observations below it. The rate was found to be greater over certain planetographic regions, but the reason for the clustering is probably that VLF signals are strongest in certain local time intervals. The rate of activity peaked at 2200 LT, decreasing toward dawn and dusk. While the occurrence rate of these active 30-s intervals cannot be compared directly with a lightning burst rate, *Russell et al.* [1989b] showed that the observed wave energy flux was consistent with lightning having a burst rate and radiated VLF energy similar to terrestrial lightning.

While the activity studies have yielded much information about the morphology of the impulsive signals, we wish to establish a new identification criterion for a lightning burst which will allow us to more accurately determine the source characteristics and occurrence distribution for comparison with terrestrial lightning. In this paper we take into account the long decay time of the instrument response and remove the effects of this decay for counting bursts. For the purposes of counting we assume that all OEFD observations in the nightside ionosphere are due to impulsive signals when deriving burst rates. We apply our improved method of counting bursts to the data of all nightside orbits of the first three seasons. These seasons have lower periapsis altitudes than the succeeding seasons. In section 2 we introduce the experimental method and describe the instrument. Then we obtain the decay constant of the instrument, and an identification criterion for bursts is developed. The statistical results are presented in section 3, including altitude, local time, and magnetic field control of burst occurrence. We also investigate the statistics of interburst timing, coincidence, and the spectral distribution. A planet-wide lightning rate is estimated and compared with that of Earth. In the last section we present some discussion and conclusions about the characteristics of the occurrence of these bursts.

## 2. Experimental Method

### 2.1. *Effect of the Decay Time of the Instrument*

As discussed by *Scarf et al.* [1980a], the Pioneer Venus orbiter (PVO) plasma wave instrument has a short dipole antenna and four band-pass channels centered at 100 Hz, 730 Hz, 5.4 kHz, and 30 kHz. The V-type antenna consists of two wire cages about 12 cm across deployed on 0.69-m booms about 0.76 m apart. The four filters have a 30% fractional frequency bandwidth. The output from each filter is passed to four continuously active automatic gain control (AGC) amplifiers which have short rise times of the order of 50 ms and much longer decay times of approximately 500 ms. The four analog voltage signals output from the AGC are converted to digital form by the spacecraft and then are telemetered to the Earth in a way that depends on the selected format and on the telemetry rate. Since the individual AGC amplifiers continuously respond to changes in the wave level input, they provide continuous information about the peak intensities, modified by the slow decay time of the AGCs. Near periapsis the spacecraft normally transmits at 1024 or 2048 bits/s, yielding two or four plasma wave scans per second.

In order to know the occurrence characteristics of VLF signals at Venus we need to make some assumptions about the duration of the OEFD input signals in the nightside ionosphere. Initially we assume that they are in the form of impulsive signals with short duration (<50 ms). From plots of the AGC output versus time we find that the decay is clearly exponential, and the time constant $\tau$ is essentially what would be expected if the input signal lasted for a short time compared to the 0.5-s decay time. A train of several bursts in rapid succession could appear as a broad peak because of the long decay time constant of the AGC amplifier. The output voltage values from the AGC are related to the electric field input to the antenna for all four frequency channels as follows:

$$E(t) = a \exp(bV(t)) \tag{1}$$

where $a$ and $b$ are constants with different values for the four channels. $E(t)$ is the input electric field (V/m/Hz$^{1/2}$), and $V(t)$ is the AGC output voltage, which is telemetered to the Earth.

From the two examples published by *Scarf et al.* [1980b] we know that the AGC response decays exponentially, and we assume an AGC response function of the form

$$V = V_0 \exp(-\Delta t/\tau) + V_{\text{off}} \tag{2}$$

where $V_0$ is the initial peak value, $V_{\text{off}}$ is an offset voltage corresponding to some ambient instrument noise level, and $\Delta t$ is the time between samples. We must determine both $V_{\text{off}}$ and the decay constant $\tau$ to use this model. The decay constant may be calculated from the successive voltage values following a large isolated noise burst, and from analysis of several individual bursts we find $\tau = 0.5$ s. Figure 1 is an example of an input burst which is tested using the model. This example of the amplitude versus time indicates that the actual signal from an isolated burst decays slightly faster than our model (dashed line). Since we identify bursts by determining if the signal is larger than that predicted by our assumed AGC decay constant $\tau = 0.5$ s, the figure shows that the model is conservative in identifying bursts. In order to prevent background noise and small bursts from being counted, we also set a threshold voltage level $V_{\text{th}}$, and we only consider those bursts with voltages which are greater than $V_{\text{th}}$.

### 2.2. *The Identification Criteria for Bursts*

The combination of the long decay constant of the AGCs and the length of time between samples masks the spaces between bursts, making it difficult to determine the real number of bursts. This is demonstrated schematically in Figure 2. Figures 2a, 2b, and 2c show how short-duration bursts of noise occurring at Venus would be measured by the OEFD and telemetered to the Earth. We see that when closely spaced burst signals (shown as equivalent AGC output voltage) enter the instrument (Figure 2a) the output signals become continuous (Figure 2b). Although many bursts may cause jumps in instantaneous output voltage because of the very short rise time of the instrument, it is very difficult to extract all these bursts from the data telemetered to the Earth (Figure 2c) because of the low telemetry rate of 4 Hz. For example, in Figure 2c we can observe only three bursts, with voltage peaks at $V_1$, $V_4$, and $V_6$. It is difficult to find the other three bursts from the data displayed in Figure 2c, since the spaces between them have been masked by the slow AGC voltage recovery.

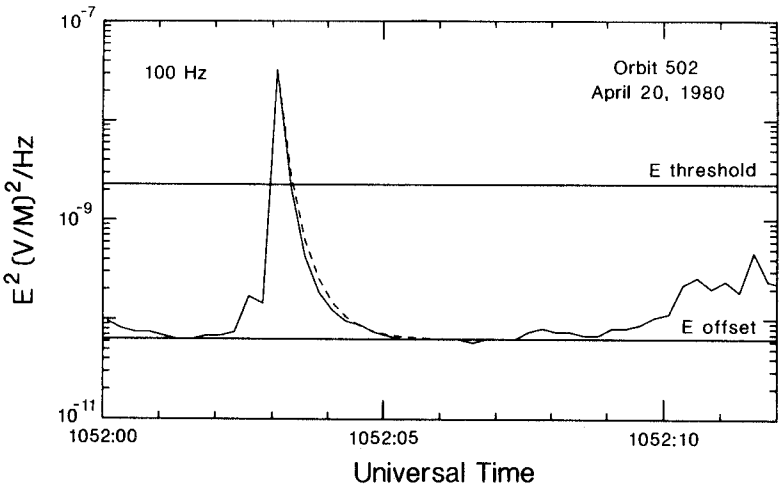


Fig. 1. An example of the burst response for orbit 502. This shows that the 100-Hz burst signal decreases more quickly than the exponential model used (dashed line), ensuring that the model is conservative when determining bursts. Threshold and offset electric field levels are also marked.

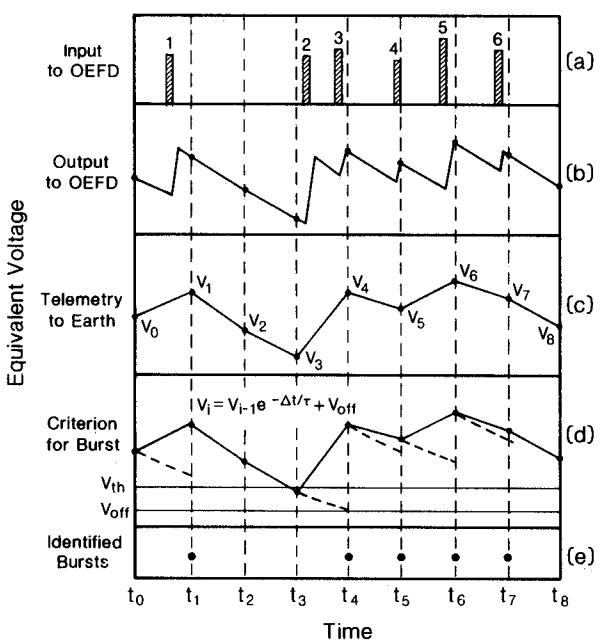


Fig. 2. Schematic of the effect of instrument sampling rate and response decay on the telemetered data stream for the OEFD. The long decay constant of the instrument masks the space between bursts and makes it difficult to determine the number of bursts. (a) A sequence of bursts assumed to be input to the OEFD, plotted as the equivalent output voltage of the instrument automatic gain controller (AGC). (b) The output of the AGC is a continuous response to the input signals modified by an exponential decay. (c) The AGC output is telemetered to the Earth at rate of 2 or 4 per second. (d) We use the formula shown to identify bursts. If the signal is greater than the predicted decay value, we define it as a burst. (e) Five of the six bursts assumed input to the OEFD have been identified.

However, with some care, it is possible to improve the burst count for high-resolution electric field data. With knowledge of the instrument response we can develop a method to remove the effect of signal decay from the data, and make a better estimate of the original input burst signals from the recorded data with 0.25 or 0.5 s resolution. We establish the burst identification criteria as follows: if the signal does not decay as fast as it should between samples, we assume that a new signal has entered the instrument.

We can use Figures 2d and 2e to explain how this procedure works. The formula in the figure shows the criterion we use to identify a burst. We set $V_{th} > V_{off}$. If signal voltage $V_i$ at time $t_i$ is greater than $V_{th}$ and the value predicted by this formula, using the signal voltage $V_{i-1}$ at time $t_{i-1}$, we identify the signal as due to a new burst. For voltage values $V_1$, $V_4$, and $V_6$, because they are obviously greater than their last respective voltage value, they must be caused by bursts entering the instrument. So we count them as three bursts, at times $t_1$, $t_4$, and $t_6$. Note that even though the voltage $V_4$ is due to two bursts rather than one, we still count only one burst because we have no way to obtain a more accurate number with the quarter-second resolution data. To show how our identification scheme gives an improved count, we consider time $t_5$. On comparison with the voltage expected for a signal decaying with the AGC constant from $V_4$, we find that $V_5$ is higher than predicted. Thus we identify a burst as having occurred. Doing a similar comparison for $V_2$, we find that the voltage $V_1$ value has decayed at the AGC rate. So no burst has occurred. Finally, of the six supposed original impulsive bursts in Figure 2a we have found five bursts in Figure 2e by applying our method. Under the assumption that bursts are of short duration and widely spaced in time our predicted rate will be close to the real burst rate. However, if the signals last much longer than we have assumed, the output voltage will be greater than the predicted decay value, resulting in an overestimate of the burst rate. On the other hand, if the burst separation is less than the sampling interval, then the burst rate will be underestimated. We cannot determine at this stage if the data are oversampled or undersampled.

As discussed above, the selection of the threshold and offset voltage values is very important. Both values of $V_{th}$ and $V_{off}$ have been obtained using several data intervals. For simplicity we have used the same value of 1.0 V as the threshold voltage for all four frequency channels. This threshold corresponds to a wave amplitude of $4.775 \times 10^{-5}$ (V/m/Hz$^{1/2}$) for the 100-Hz channel. We have chosen voltage offset values of 0.15, 0.35, 0.25, and 0.35 V corresponding to the background noise levels of the 100-Hz, 730-Hz, 5.4-kHz and 30-kHz channels respectively. We use 0.5 s as the decay time constant of the AGCs for all channels. Figure 3 shows time series of electric field data at 0.25 s resolution from orbit 501 of season 3 observed by the OEFD. We see that very strong bursts appear in all four frequency channels. All

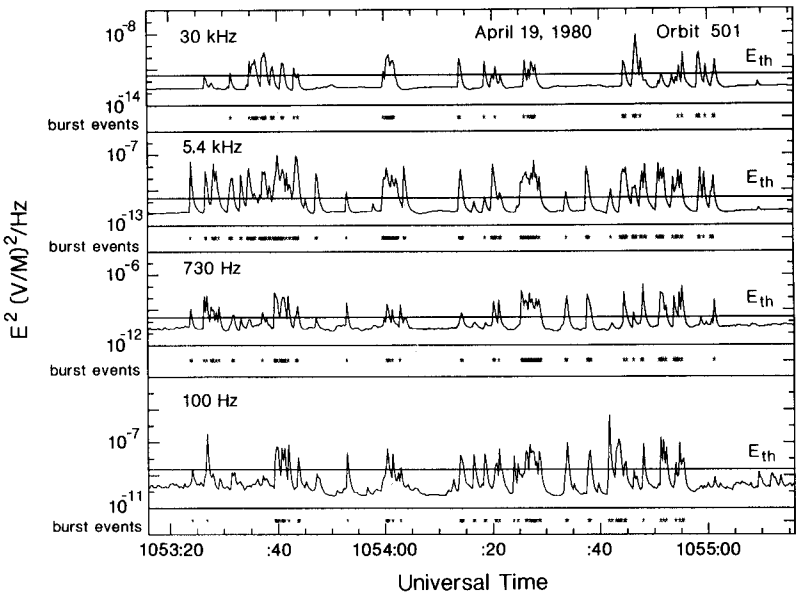


Fig. 3. Time series of 0.25-s resolution electric field data from orbit 501. The threshold values for each channel are also shown. Very strong bursts run through all four frequency channels. All impulsive signals show the characteristic decay of the AGCs. The asterisks under the electric field signals represent a wave burst as determined by the method described in the text.

impulsive signals show the characteristic decay of the AGCs. We have also marked the threshold electric field values for all four channels. The asterisks under the electric field signal in each frequency channel represent a wave burst as determined by the method described in this section. Almost every large impulsive signal includes many bursts.

Before we perform a statistical analysis on these impulses, we need to carefully screen the data for false events which are usually produced either by the slow enhancement of wave amplitude exceeding the threshold voltage level due to the interaction of the spacecraft with the neutral atmosphere near periapsis or by interference associated with the interaction of the spinning spacecraft with the ionosphere. Telemetry noise pulses are easily identified because they are not associated with signals passing through the instrument electronics and so do not show any decay. Further, they appear in magnetic field data measured simultaneously. After we obtain the total number of impulsive signals and the total time spent by the spacecraft in local time intervals and height ranges, a normalized burst rate distribution can be determined.

## 3. Statistical Results

We have used the above method of burst identification to perform a statistical study of the rate of impulsive signals observed by Pioneer Venus within the context of the lightning hypothesis. Terrestrial lightning flashes often consist of several individual strokes, but it is not clear if we can resolve an individual stroke. Because of this we have elected to refer to the signals as bursts, rather than flashes or strokes. From the report of *Scarf et al.* [1987] the largest number of bursts occurred during the first three seasons where Pioneer Venus periapsis was at its lowest altitudes. After the first three seasons the periapsis altitude was allowed to rise, and the number of events detected in the night ionosphere dropped. Thus we have selected the data from the first three seasons of nightside periapsis orbits for study. Because the occurrence rate decreases with altitude, we have restricted our study to altitudes below 300 km. Data are available at low nightside altitudes for the first three seasons, corresponding to orbits 025–125, 250–350, and 470–570. Unfortunately, Venus passed through superior conjunction in season 2, and no data are available for orbits 250–285. Furthermore, when Venus was furthest from the Earth, the telemetry rate was lower. The data studied here were obtained with two different temporal resolutions: 0.5 s and 0.25 s.

### 3.1. *Altitude and Local Time Distributions*

When we normalize the burst number by time spent, we find that burst rates are generally lower for 0.5-s resolution than 0.25-s resolution data because the former have lower temporal resolution. In order to obtain the altitude distribution of the burst rate averaged over three seasons for the four frequency channels we need to correct the burst rate obtained with low-resolution data before merging it with high-resolution data. The correction factor is estimated two ways. First, on comparing the burst rates of the two different resolution data as a function of altitude we find that the 0.25-s resolution data have a factor of 1.38 larger burst rate than the 0.5-s resolution data. Second, as discussed in section 3.3, we can calculate a correction factor using the burst separation statistics. This yields a correction factor of 1.42, and we use the average of these two methods (i.e., 1.40) to correct the lower-resolution data. The combined rate ($r$) is given by $r = (n_{0.25} + 1.40n_{0.5})/(t_{0.25} + t_{0.5})$, where $n_{0.25}$ and $n_{0.5}$ are the number of bursts for the different resolutions and $t_{0.25}$ and $t_{0.5}$ are the time spent.

Figure 4 gives the altitude distribution of the burst rates at the four frequencies for the first three seasons. The burst rates are determined in 10-km intervals as a function of altitude from 140 km to 300 km. Rates are obtained by dividing the number of bursts by the time spent in each altitude interval, after correcting for the different temporal resolution as discussed above. From Figure 4 we can see that burst rates for all frequencies have a general decreasing trend with increasing altitude, although the rates for the two higher frequencies appear to decrease at the lowest altitude. The burst rate at 100 Hz has a maximum of 0.13/s at 160–170 km and then decreases with increasing altitude. At 150–160 km the rates of 5.4 kHz and 30 kHz peak, but

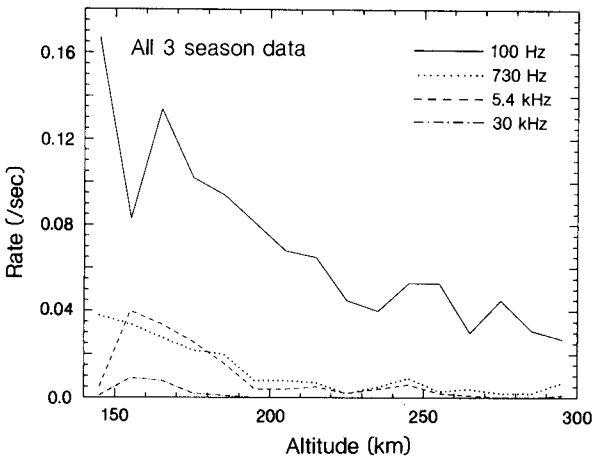


Fig. 4. Altitude distribution of burst rates at the four frequencies for the first three seasons, in each 10-km altitude bin, for altitudes in the range 140–300 km. The burst rates are obtained by merging the different resolution data after correcting the 0.5-s resolution data. Burst rates generally decrease with increasing altitude. The 100-Hz maximum burst rate is 0.13/s.

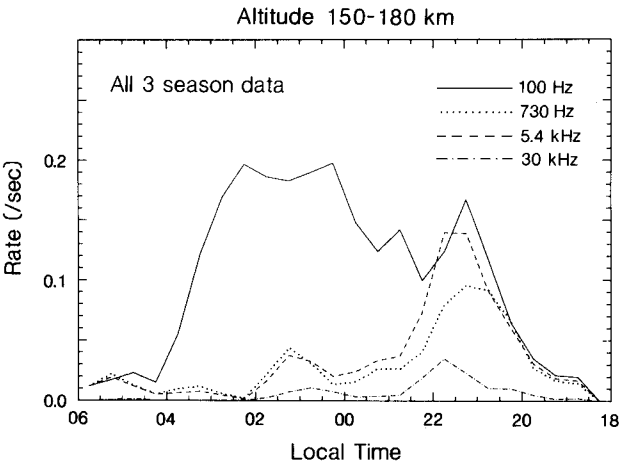


Fig. 5. Burst rates versus local time for all four channels between 150 and 180 km in altitude. The 100-Hz signals partially peak before midnight, but the maximum appears after midnight. Higher-frequency signals clearly peak at 20–22 LT. The correlation of burst rates with local time confirms that there is a significant wideband source after dusk.

the rate at 100 Hz decreases. At the lowest altitude the 730-Hz rate reaches its maximum, and the 100-Hz rate also increases again.

The fact that burst rates generally decrease with increasing altitude suggests that there is a source below the ionosphere. The 100-Hz signals which are generated by this source can propagate as whistler mode waves, suffering some attenuation due to electron Landau damping and gyrodamping [*Strangeway*, 1990]. The signals above the electron gyrofrequency will be rapidly attenuated as they penetrate the ionosphere. So the rates for higher frequencies fall rapidly with increasing altitude. Our normalized burst rate results provide further support for the previous studies of altitude dependence [*Scarf et al.*, 1987; *Russell et al.*, 1988a, b].

In Figure 4 the burst rate is maximum in the 150–180 km altitude range, and we shall restrict the data to this range when calculating the burst rate as a function of local time, as shown in Figure 5. These rates have been corrected for different temporal resolution and smoothed with a weighted running average over three adjacent local time bins. From Figure 5 we can see that 100-Hz signals have some activity at 21–23 LT but the maximum rate occurs in the postmidnight local time sector. The higher-frequency signals have a maximum at 20–22 LT and decrease toward dawn and dusk. The largest rate in the higher-frequency channels is 0.14/s, and occurs in the 5.4-kHz channel. The higher-frequency signals all seem to come from the same source. After midnight around 00–03 LT, mainly 100-Hz signals appear, and the burst rate reaches a maximum of 0.20/s. This high rate may be due to oversampling of the 100-Hz signals. If a natural impulsive signal has a finite duration, then a single impulse may be counted twice or even more times. This postmidnight 100-Hz burst rate peak did not appear in the results of *Russell et al.* [1988c, 1990], who counted the number of times a 30-s interval had any activity rather than the number of impulses in that interval. Figure 5 confirms that the signals have a clear correlation with local time. The premidnight wideband peaks are qualitatively consistent with results of *Russell et al.* [1988c, 1989a].

Since we have restricted the local time analysis to altitudes below 180 km, each orbit only covers 10–20 min of local time, while the local time of periapsis drifts by about 6 min per orbit. Consequently, a value in a local time bin of Figure 5 should consist of bursts from six or so orbits. We find that there is a noticeable variation in burst rate from orbit to orbit, with some orbits displaying no activity, while other orbits contain many strong bursts. However, the fluctuations in burst rate do not seem to be related to the periodic changes in periapsis altitude which occurred throughout seasons 1–3, as the periapsis altitude was maintained on average around 150 km through periodic altitude adjustments. Moreover, the orbit to orbit variation in activity does not appear to depend in an obvious manner on the ionospheric properties. Consequently, we have not removed any data from the statistics, but rather have reduced the fluctuations in the local time distribution through the running average.

### 3.2. *Magnetic Field Control*

We have also investigated the influence of magnetic field strength on the burst rates for all four frequencies. Figure 6 shows the burst rate versus the magnetic field strength $B$ for all three seasons with altitude between 150 and 180 km. In the top panel we also show the $B$ distribution in this altitude range. The average $B$ is about 18 nT, corresponding to the electron gyrofrequency $f_c = 500$ Hz. If the waves in the 100-Hz channel are whistler mode waves, we expect that the variation of the magnetic field should have greater influence on 100-Hz signal propagation since the gyrofrequency is the upper cutoff frequency for whistler waves. The results in Figure 6 show that the burst rate at 100 Hz for all three seasons has a strong positive correlation with $B$. In contrast, the three higher-frequency rates are less sensitive to the field strength. These results suggest that the higher frequencies may have a different propagation mechanism than the 100-Hz signals. The correlation of the 100-Hz signals with the magnetic field is consistent with whistler mode propagation.

The dependence on magnetic field strength shown in Figure 6 has some differences from the previous results of *Russell et al.* [1988c]. In their studies, which used different local time and altitude ranges, the rate of activity of the three higher-frequency channels decreased quickly as the magnetic field strength decreased. In addition, they found that the 100-Hz activity appeared to depend only weakly on magnetic field strength. The strong dependence on magnetic field strength for the 100-Hz burst rate shown in Figure 6 is also found if we restrict the data

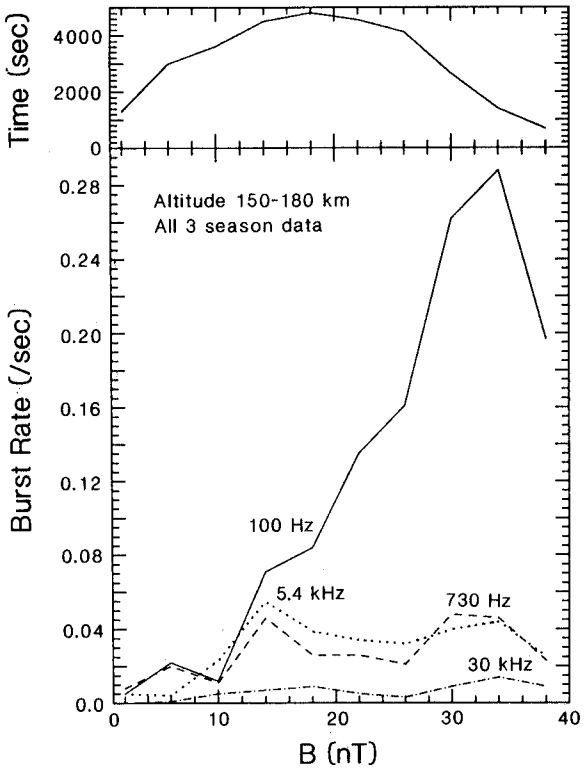


Fig. 6. Magnetic field control of burst rates for all three seasons of data between altitudes 150 km and 180 km. The top panel shows the significance of our statistics by plotting the total sampling time with variation in magnetic field strength. The average magnetic field strength is about 18 nT. We see that the burst rate at 100 Hz shows a strong correlation with increasing magnetic field, as opposed to little or no correlation in the three higher-frequency channels. This provides further evidence that 100-Hz signals propagate in the whistler mode.

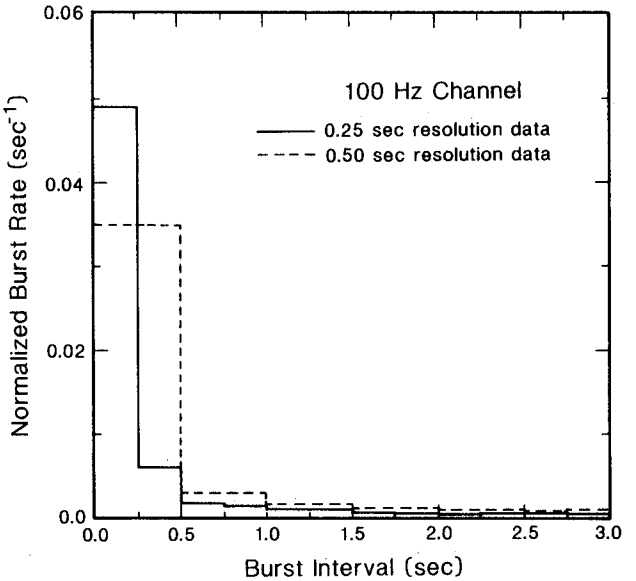


Fig. 7. Normalized 100-Hz burst interval histogram for 0.25-s (solid line) and 0.5-s (dashed line) resolution data. Although many of the 0.25-s resolution data bursts have intervals <0.25 s, 40% of the bursts have intervals >0.25 s. Comparison of burst rates at different time intervals can be used to obtain a correction factor for merging the 0.5-s resolution data with the 0.25-s resolution data.

to the same altitude and local time range used by *Russell et al.* [1988c] (19–22 LT, 160–225 km altitude). The difference may be due to the different statistical methods used, with the 30-s occurrence rate studies underestimating the burst rate. In accord with this suggestion, examination of the data indicates that 100-Hz activity in high magnetic fields is often quasi-continuous. This would give many bursts in our present study, but would only give one count for each 30-s interval in the study of *Russell et al.* [1988c].

### 3.3. *Burst Interval and Coincidence*

As part of this study we have also examined the statistics of the interval between successive bursts. We emphasize that this analysis depends on the assumption that all signals are impulsive in nature. If the waves have a finite duration, they may be counted twice by our technique, while those signals with duration greater than the sampling time will always be counted twice. Figure 7 is a histogram of the 100-Hz burst interval distribution. In order to make a comparison of 0.25-s with 0.5-s resolution data we normalize the burst number by total time spent observing at each time resolution. The number of events is plotted as a function of the time interval between successive bursts. We see that burst numbers decrease steeply as the interval between bursts increases. The three higher-frequency channels have a similar distribution of intervals between bursts. From Figure 7 we see that although the number of bursts with 0.25-s spacing is large, this number is still less than 60% of the total number of bursts. Consequently, over 40% of all bursts counted are clearly separated impulsive signals rather than possible continuations of the preceding detected burst. For those signals with a spacing of 0.25 s we cannot know the kind of distribution bursts would take in this interval because of the limited temporal resolution. We note that at the Earth many flashes occur in rapid succession, so that the VLF signal would appear continuous at 0.25 s resolution. If the source at Venus also consists of many closely spaced flashes, then our method underestimates the burst rate. On the other hand, if the source spectrum consists of relatively long pulses, then we overestimate the burst rate. Hence the burst rate depends on the sampling time of the data, and as noted in section 3.1, the burst rate for higher-resolution data is greater than for lower-resolution data.

In the previous sections we used a correction factor of 1.40 to merge 0.5-s resolution data with 0.25-s resolution data. This factor was obtained through a combination of regression analysis and consideration of the burst distribution shown in Figure 7. The correction factor can be obtained as follows. On the average, 50% of the bursts separated by <0.25 s will be counted as a pair of bursts separated by <0.5 s when sampled at 0.5 s resolution. We assume that $2x$ bursts occur <0.25 s after the previous burst, and $y$ bursts are separated by >0.25 s. The total number of bursts will be $2x + y$ at 0.25 s resolution and $x + y$ at 0.5 s resolution. We can correct the burst rate for closely spaced bursts using the factor $(2x + y)/(x + y)$. From Figure 7, $2x = 0.050T$, and $y = 0.035T$, where $T$ is the total time spent, giving a correction factor of 1.42 from analysis of the burst separation.

With our burst identification method we can also determine the degree of coincidence between bursts in the different frequency channels. In particular, we can determine if the bursts are broadband or narrowband in nature. The results of our analysis of burst coincidence are shown in Table 1. For each channel we determined if the burst was detected in isolation, or if the burst was coincident with a burst in at least one other channel. The latter are labeled "multichannel" in the table. We show the actual number of bursts as an indication of the statistical significance of the results for each channel.

TABLE 1. Coincidence of Burst Occurrence for the Four Frequency Channels

| Channel | Isolated | Multichannel |
|---|---|---|
| 100 Hz | 3666 (91.5%) | 341 (8.5%) |
| 730 Hz | 388 (43.9%) | 496 (56.1%) |
| 5.4 kHz | 406 (49.6%) | 413 (50.4%) |
| 30 kHz | 24 (16.8%) | 119 (83.2%) |

Table 1 clearly shows that the 100-Hz signals are dominated by bursts which occur only in the 100-Hz channel. For the higher frequencies, there is a mixture of both. If we consider the 30-kHz channel, arguing that this channel best shows the spread to high frequencies, then we see that a 30-kHz burst rarely occurs in isolation. That the 730-Hz and 5.4-kHz channels show a mixture of both isolated and multichannel bursts may be a consequence of the source spectrum for the waves. *Scarf et al.* [1980b] noted that for terrestrial lightning the peak power in the VLF range is at 5 kHz, with the power falling off as $f^{-2}$. While the peak frequency may be different at Venus, we might expect a similar spectral slope at the higher frequencies. In Figure 3, the intensity threshold for our burst identification decreases roughly as $1/f$, and weak signals which are above threshold at 5.4 kHz may consequently be below threshold at 30 kHz.

### 3.4. *Power Spectrum Distribution*

The decrease of the burst rate for the four frequency channels with increasing altitude suggests that there will also be a variation of the signal power with altitude. We have examined the altitude profile of the wave power, and Figure 8 shows the altitude variation of the average value of burst wave power (electric field amplitude squared) of 0.25-s resolution data for the four frequency channels plotted in 10-km altitude bins for altitudes 140–200 km. We have included error estimates for the mean, where larger error bars reflect lower burst number. The wave power is maximum in all the channels in the 150–170 km altitude range, with a decrease in power at both higher and lower altitudes. Except at the lowest altitude the average spectral power is at least an order of magnitude above the burst threshold, but it is likely that the spectral shape is biased by the threshold, since weak signals are excluded from the calculation of spectral power. However, the data in Figure 8 are probably adequate for determining the altitude profile of the wave intensity at each frequency.

As a possible explanation for the altitude variation we can use conservation of Poynting flux for the 100-Hz waves, as discussed by *Russell et al.* [1989b]. However, we find that the increase in wave power between 145 and 155 km altitude is larger than that expected through Poynting flux conservation. Furthermore, the variation of the higher-frequency channels cannot be explained by a Poynting flux argument, since these waves are not whistler mode.

An alternative possibility we consider here is that the rise time of the electric discharge is too rapid at lowest altitude for proper detection by the instrument while at higher altitudes the electric pulse has become somewhat broadened through dispersion. The OEFD AGCs have rise times of the order of 50 ms [*Scarf et al.*, 1980a], and any impulse of much shorter duration would probably not be detected. We can estimate the amount of dispersion for whistler mode waves using the difference in group velocity ($v_g$) over the 100-Hz channel bandwidth (30%). For low-frequency whistlers ($f \ll f_c$), $v_g/c \approx 2\sqrt{(ff_c)}/f_p$. Assuming the magnetic field strength is 20 nT and the average plasma density is $10^3$ cm$^{-3}$, then signals measured by the 100-Hz channel will

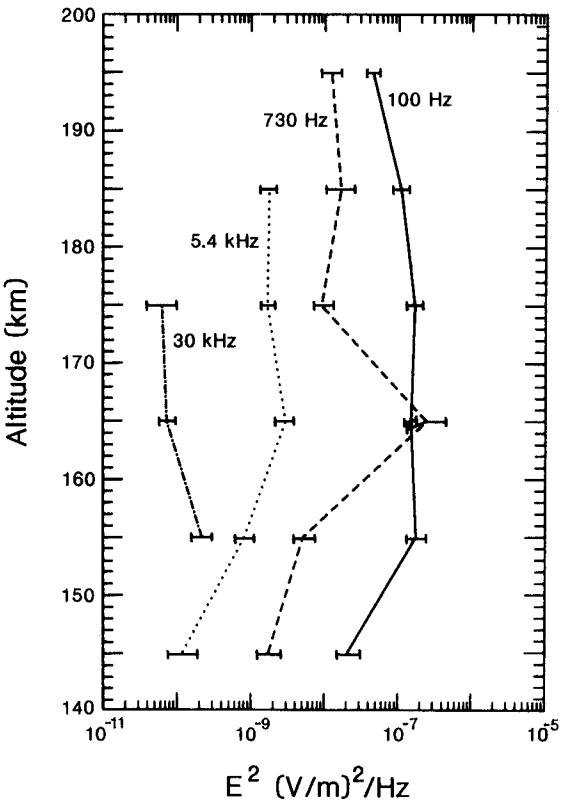


Fig. 8. Altitude variation of the average value of burst wave power of 0.25-s resolution data for four frequency channels between 140 and 200 km in 10-km altitude bins. The signal wave power is maximum at 160–170 km for 730 Hz and 5.4 kHz and at 150–160 km for 100 Hz and 30 kHz. The error of the mean is shown for each channel. Mean intensities are not shown for altitude bins containing less than three bursts.

have broadened by 15 ms after traveling 50 km. This is much less than the sampling time of the instrument, but only a factor of 3 less than the AGC rise time. Consequently we would not expect any broadening of the signal due to dispersion to affect the burst rate calculation through oversampling, provided the signal is above threshold. On the other hand, there is some possibility that the broadening may increase the probability of detection at higher altitudes by allowing the AGC output to rise above threshold, and so the bursts may be undersampled at lowest altitude. However, a more detailed study of the OEFD response to impulsive signals is necessary to adequately address this point.

A decrease in intensity might be expected at higher altitudes, as the waves are likely to be attenuated as they propagate away from the source. Consequently, whether or not the decrease of wave intensity at lowest altitude is due to changes in the instrument response or an intrinsic property of the waves is an important question. However, as mentioned above, because of the dispersion in the ionosphere, rapid signals from the atmosphere which may be too short to be detected at lowest altitude will be lengthened with increasing altitudes and become detectable.

### 3.5. *Planet-Wide Rate*

Using the results of the previous sections, we can estimate the planet-wide lightning rate at Venus and compare this with terrestrial lightning. However, this estimate will be a function of the area of the planet's surface from which VLF signals may reach the spacecraft at any one time. There are no studies which can determine the area of the planet monitored by the VLF receiver, and we have no knowledge of the size of the discharge which

could be detected at the OEFD. Therefore we must make some assumptions in order to obtain an estimate of the planet-wide lightning rate at Venus.

Because the cloud layer at Venus is as high as 50 km altitude, any lightning on Venus would be expected to be an intracloud discharge phenomenon and not cloud to ground. PVO periapsis is near 150 km and is consequently at least 100 km distance away from the cloud layer. For the purpose of our calculation we assume that PVO can detect as far horizontally as the spacecraft is distant vertically. We assume, then, that any burst detected by PVO comes from a circular region of 100 km radius. Since the local time and latitudinal extent of lightning is not well known, we must also make some assumptions on the size of the active region. We will assume that lightning is restricted to equatorial latitudes less than ±30°. Since solar heating is likely to be responsible for lightning, we expect lightning to occur in the dayside. However, the OEFD only detects bursts in the nightside. VLF signals due to lightning may not be detected on the dayside because of the higher instrument noise levels. We consequently take two limits for the local time distribution of lightning, assuming that lightning occurs in the range 18–24 LT only or in the range 12–24 LT. Together with the restriction in latitude, these local time ranges correspond to 1/8 and 1/4 of the planet surface respectively. Higher-frequency signals better reflect local source activity since the 100-Hz waves may have propagated some distance from the source, and we use the maximum burst rate 0.14/s at 5.4 kHz around 21–22 LT in Figure 5 as the lightning occurrence rate over the locally active region. We calculate the maximum planet-wide burst rate as 250/s for 1/8 of the planet and 500/s for 1/4 of the planet. This is larger than the terrestrial global flash rate of about 100/s, but our rate depends strongly on the area over which the OEFD is sensitive to a lightning burst. A factor of 2 increase in this assumed area will halve the global rate.

Our burst rate of 0.14/s over 31,400 km$^2$ area is equivalent to a local burst rate of 140/km$^2$/terrestrial year. Based on the statistics of Venera spacecraft observations, *Krasnopolsky* [1983] estimated that there were about 700 flashes/s occurring on Venus, corresponding to a global flash rate of about 45/km$^2$/terrestrial year. *Russell et al.* [1989b] also estimated from the calculation of the 100-Hz Poynting flux that a lightning source rate of 80 flashes/s Venus-wide would be sufficient to power the VLF emission. Our maximum rate of 140 bursts/km$^2$/terrestrial year is much larger than the 2.7 bursts/km$^2$/terrestrial year estimated by *Scarf and Russell* [1983] because events identified by them could last many seconds and hence contain many bursts.

## 4. Discussion and Conclusions

The temporal resolution of the data limits the accuracy of estimates of burst rate since the maximum rate obtained by our method is 4.0/s with 0.25-s resolution data. We cannot determine the detailed interval distribution of those bursts with intervals between 0.0 and 0.25 s. Also we cannot distinguish closely spaced bursts from continuous emissions. In addition, our definition of a burst is strongly dependent on the threshold value we choose. When we use a lower threshold level, we will get a larger burst count. Since our results come from the statistics of a random event, the accuracy should depend on the number of bursts detected, and hence on the time spent by the spacecraft in a particular altitude or local time interval. At lowest altitude our results have less accuracy since the statistics are less significant.

With respect to local time, we find that the waves are wideband in the premidnight local time sector, but signals consist mainly of 100-Hz low-frequency waves after midnight. The larger postmidnight 100-Hz burst rate peak possibly includes the effect of oversampling as mentioned before. This local time distribution can be explained in two ways. First, there may be a wideband source which occurs mostly at about 2200 LT. Waves from this source directly penetrate the ionosphere by some anomalous transmission mechanism as a "near field". The 100-Hz waves can propagate with little damping in the waveguide between the ground and the ionosphere to postmidnight local times and then pass through the ionosphere as a "far field". This mechanism requires conditions which favor 100-Hz wave penetration in the postmidnight ionosphere. A preliminary survey shows that while plasma density holes occur throughout the nightside ionosphere, the distribution of holes is asymmetrical about midnight, extending further into the postmidnight sector [*Brace et al.*, 1982]. The holes seem to play an important part in the transmission of 100-Hz waves. A second explanation is that waves before and after midnight have two different sources. The postdusk source has a very wide frequency spectrum while the near-midnight source is only at low frequencies. However, the wideband source cannot be explained as Doppler shift of acoustic mode waves since there is no local time dependence on the orientation of the spacecraft velocity vector and the magnetic field that is sufficient to explain the confinement to the postdusk local time sector. It is not apparent why an ionospheric source should have the local time dependence observed. On the other hand, only whistler mode waves below the electron gyrofrequency would have access to the spacecraft in a homogeneous collisionless plasma. It is still a mystery how the high-frequency signals enter the ionosphere.

With regard to the 100-Hz signal, *Taylor et al.* [1985] noted that the 100-Hz bursts often occurred at the time of a depression in plasma densities they called a trough or a hole. They suggested that it was likely that some in situ plasma instabilities in the vicinity of troughs, such as the ion acoustic wave, resulted in these burst signals, but because of the lower density and stronger magnetic field inside a hole, it may also trap and guide VLF waves. Terrestrial studies have shown that density irregularities can cause ducting of VLF waves. *Scarf and Chappell* [1973] found that most VLF signals were observed in density enhancements while a few signals corresponded to density troughs. *Carpenter et al.* [1981] reported that both density troughs and crests with ±30% density variation can duct whistlers in the plasmasphere. In the Venus nightside ionosphere there are many density holes instead of density enhancements. The magnetic field usually increases 2 – 10 times and the plasma density drops by about an order of magnitude inside holes. Both changes have a consistent effect to cause a significant increase of phase velocity of whistler mode waves. Consequently, a spacecraft might detect stronger electric field signals in these holes, through ducting and through conservation of wave Poynting flux.

When the 100-Hz signals propagate through the ionosphere in the form of whistlers, dispersion will occur. As discussed previously, we might expect dispersion to broaden the signal by about 15 ms on traveling 50 km. This duration is much less than the data sample rate and somewhat shorter than the rise time of the AGCs. Except perhaps at the lowest altitude, where AGC rise time effects may be important, we would not expect the dispersion to be significant for the data used in this study. However, it is possible that the dispersion can cause significant broadening of impulsive signals at higher altitudes (>300 km).

It is also not clear whether the whistler mode waves have enough energy to penetrate the ionosphere and reach to the spacecraft or not. We need to calculate how wave energy is

transmitted in a stratified plasma medium. Analyses show that it is very difficult for whistler waves to propagate vertically when the ambient magnetic field is horizontal. Furthermore, an accurate calculation of wave transmission needs more information, such as how much energy is released by the lightning discharges, source power spectrum distribution, electron concentration of the nightside ionosphere below 150 km, and ionospheric conductivity structure. At present we do not have any detailed knowledge of these parameters.

In summary, from analysis of the first three seasons of nightside data we obtain the following morphological characteristics of the occurrence of VLF bursts at Venus:

1. The burst rates for all four frequency channels reach maximum below 160 km in height. The burst rates decrease with increasing altitude. The 100-Hz low-frequency signals partially peak at 21–22 LT, but the maximum appears after midnight, with a peak rate of 0.20/s. The higher-frequency signals peak at 20–22 LT and decrease toward dawn and dusk, with the highest rate of 0.14/s being detected in the 5.4-kHz channel. The burst rates vary from orbit to orbit.

2. The burst rate for the 100-Hz channel has a strong dependence on the magnetic field strength, but for the other three higher-frequency channels the rates are less sensitive to field strength. The different magnetic field dependence provides further evidence that 100-Hz signals propagate in the whistler mode. Higher-frequency waves probably have different modes and propagation mechanisms.

3. The number of bursts decreases steeply as the time interval between one burst and the previous burst increases. Nearly 60% of the total bursts at 0.25 s resolution are less than 0.25 s away from the previous burst. At 100 Hz, 91.5% of the bursts are narrow-band signals, appearing in the 100-Hz channel only, while 16.8% of the 30-kHz bursts are isolated. This is consistent with a narrow-band source for the 100-Hz waves and a broadband source for the higher frequencies.

4. The VLF wave power is maximum between 150 and 170 km. While the increase in refractive index due to the higher plasma density may contribute to the intensity falloff at the lowest altitudes for the 100-Hz signals, it is more likely that the change in instrument response contributes to the change in intensity. However, further study is necessary.

5. We estimate the peak local lightning rate to be 140/km$^2$/terrestrial year, which gives a global flash rate of 250/s, assuming lightning occurs over 1/8 of the planet surface. The global flash rate is proportional to the assumed active area. Our rate is comparable to or larger than the terrestrial rate of lightning. This rate is greater than rates previously estimated by *Scarf and Russell* [1983] but similar to those estimated from optical observation by *Krasnopolsky* [1983].

In conclusion, any postulated source for the observed waves must explain the impulsive structure of the bursts and naturally produce the local time variation and magnetic field control of low-frequency wave burst rates. It is our opinion that lightning occurring in the atmosphere of Venus is the most likely candidate to explain the observations presented here.

*Acknowledgments.* When using the Pioneer Venus OEFD data we cannot help but express our respect and gratitude to the late Frederick L. Scarf who was the Principal Investigator for the OEFD. One of the authors (C.-M. H.) also wishes to thank Gordon Maclean for his help in computer programming. This work was supported by NASA under grants NAG2-485 and NAG2-501. This is IGPP publication 3426.

The Editor thanks two referees for their assistance in evaluating this paper.

## REFERENCES

Brace, L. H., R. F. Theis, H. G. Mayr, S. A. Curtis, and J. G. Luhmann, Holes in the nightside ionosphere of Venus, *J. Geophys. Res.*, *87*, 199–211, 1982.

Carpenter, D. L., R. R. Anderson, T. F. Bell, and T. R. Miller, A comparison of equatorial electron densities measured by whistlers and by a satellite radio technique, *Geophys. Res. Lett.*, *8*, 1107–1110, 1981.

Krasnopolsky, V. A., Lightning and nitric oxide on Venus, *Planet. Space Sci.*, *31*, 1363–1369, 1983.

Russell, C. T., Venus lightning, *Space Sci. Rev.*, *55*, 317–356, 1991.

Russell, C. T., and F. L. Scarf, Evidence for lightning on Venus, *Adv. Space Res.*, *10(5)*, 125–136, 1990.

Russell, C. T., and R. N. Singh, A re-examination of impulsive VLF signals in the night ionosphere of Venus, *Geophys. Res. Lett.*, *16*, 1481–1484, 1989.

Russell, C. T., M. von Dornum, and F. L. Scarf, The altitude distribution of impulsive signals in the night ionosphere of Venus, *J. Geophys. Res.*, *93*, 5915–5921, 1988a.

Russell, C. T., M. von Dornum, and F. L. Scarf, Planetographic clustering of low-altitude impulsive electric signals in the night ionosphere of Venus, *Nature*, *331*, 591–594, 1988b.

Russell, C. T., M. von Dornum, and F. L. Scarf, VLF bursts in the night ionosphere of Venus: Effects of the magnetic field, *Planet. Space Sci.*, *36*, 1211–1218, 1988c.

Russell, C. T., M. von Dornum, and F. L. Scarf, Source location for impulsive electric signals seen in the night ionosphere of Venus, *Icarus*, *80*, 390–415, 1989a.

Russell, C. T., M. von Dornum, and R. J. Strangeway, VLF bursts in the night ionosphere of Venus: Estimates of the Poynting flux, *Geophys. Res. Lett.*, *16*, 579–582, 1989b.

Russell, C. T., M. von Dornum, and F. L. Scarf, Impulsive signals in the night ionosphere of Venus: Comparison of results obtained below the local electron gyro-frequency with those above, *Adv. Space Res.*, *10(5)*, 37–40, 1990.

Scarf, F. L., and C. R. Chappell, An association of magnetospheric whistler dispersion characteristics with changes in local plasma density, *J. Geophys. Res.*, *78*, 1597–1602, 1973.

Scarf, F. L., and C. T. Russell, Lightning measurements from the Pioneer Venus orbiter, *Geophys. Res. Lett.*, *10*, 1192–1195, 1983.

Scarf, F. L., and C. T. Russell, Evidence of lightning and volcanic activity on Venus: Pro and con, *Science*, *24*, 222–224, 1988.

Scarf, F. L., W. W. L. Taylor, and P. F. Virobik, The Pioneer Venus orbiter plasma wave investigation, *IEEE Trans. Geosci. Remote Sens.*, *GE-18*, 36–38, 1980a.

Scarf, F. L., W. W. L. Taylor, C. T. Russell, and L. H. Brace, Lightning on Venus: Orbiter detection of whistler signals, *J. Geophys. Res.*, *85*, 8158–8166, 1980b.

Scarf, F. L., K. F. Jordan, and C. T. Russell, Distribution of whistler mode bursts at Venus, *J. Geophys. Res.*, *92*, 12407–12411, 1987.

Singh, R. N., and C. T. Russell, Further evidence for lightning on Venus, *Geophys. Res. Lett.*, *13*, 1051–1054, 1986.

Strangeway, R. J., Radioemission source disputed, *Nature*, *345*, 213–214, 1990.

Strangeway, R. J., Plasma waves at Venus, *Space Sci. Rev.*, *55*, 275–316, 1991.

Taylor, H. A., Jr., and P. A. Cloutier, Telemetry interference incorrectly interpreted as evidence for lightning and present-day volcanism at Venus, *Geophys. Res. Lett.*, *15*, 729–732, 1988.

Taylor, H. A., Jr., J. M. Grebowsky, and P. A. Cloutier, Venus nightside ionospheric troughs: Implications for evidence of lightning and volcanism, *J. Geophys. Res.*, *90*, 7415–7426, 1985.

Taylor, W. W. L., F. L. Scarf, C. T. Russell, and L. H. Brace, Evidence for lightning on Venus, *Nature*, *279*, 614–616, 1979.

C.-M. Ho, C. T. Russell, and R. J. Strangeway, Institute of Geophysics and Planetary Physics, University of California, Los Angeles, CA 90024.

(Received September 20, 1990;
revised July 1, 1991;
accepted July 23, 1991.)